FEMTOSECOND ELECTRON BEAM AND X-RAY BEAMS AT THE LINAC COHERENT LIGHT SOURCE*

Y. Ding, A. Brachmann, F.-J. Decker, P. Emma†, C. Field, J. Frisch, Z. Huang, R. Iverson, H. Loos, H.-D. Nuhn, D. Ratner, J. Turner, J. Welch, J. Wu, F. Zhou
SLAC National Accelerator Laboratory, Menlo Park, CA 94025, USA

Abstract

Generation of ultrashort x-ray pulses (femtoseconds to attoseconds) is attracting much attention within the x-ray FEL user community. At the Linac Coherent Light Source (LCLS), we have successfully delivered femtosecond x-ray pulses to the users with two operating modes – low-charge (20-40pC) scheme and emittance spoiling foil method. Diagnostics on the femtosecond beams is also a challenging topic and good progresses have been made at LCLS. In this paper we report the experimental studies on the two femtosecond operation schemes, the x-ray performance and also the diagnostic progress.

INTRODUCTION

The realization of x-ray free-electron lasers (FEL) has opened up vast opportunities for scientific research. At the Linac Coherent Light Source (LCLS) [1], normal operation with a charge of 150-250pC can produce x-ray pulses from tens of femtoseconds (fs) to a few hundred fs. At the same time, there is a high interest to produce even shorter x-ray pulses, down to fs or even sub-fs regime. We have developed two operation modes to generate shorter x-rays at LCLS. One method is to reduce the bunch charge and hence the bunch length (e.g., from 150-250 pC to 20 pC). The resulting x-ray pulse is expected, and in some cases confirmed, to be less than 10 fs [2, 3]. Another method is to use an emittance-spoiling foil (a slotted foil), which spoils the emittance of most of the beam and leaves a small temporal fraction to lase. Both of the two schemes have been widely used in user experiments, and we will describe the operational performance of these two schemes, and also discuss the recent diagnostic progress.

LOW CHARGE OPERATION

Reducing the charge from 150pC to 20pC at LCLS, we adjust the UV laser spot diameter at the cathode from 1mm to 0.6mm, and the laser pulse duration is about 4ps fwhm. Setting the photoinjector gun rf phase w.r.t laser at -15°, the typical e-beam bunch length in the injector is measured with a transverse deflector at about 210 μm rms, and the sliced emittance is about 0.14μm. The laser heater is typically switched off during low-charge operation. This low-emittance beam with a shorter initial bunch makes it possible to achieve a higher brightness e-beam at the end of the linac compared with the high-charge mode.

The low-charge electron bunch after the injector is then accelerated in the SLAC linac and compressed twice in BC1 at 220 MeV and in BC2 at 5 GeV. After BC2, the bunch can be further accelerated in L-3 linac to get a maximum energy of 14.6 GeV, or decelerated to get a low energy beam of 3.5 GeV, for FEL lasing at different wavelengths from 1.3 to 24 Å. An even lower energy down to 2.5 GeV has also been recently studied [4]. The machine configuration is shown in Fig. 1.

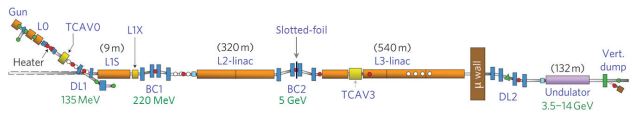

Figure 1: LCLS machine layout. The slotted-foil is at the middle of BC2.

Hard x-ray FELs at 20pC

The low-charge bunch is finally compressed in BC2 to reach kA-level current. Although both the R_{56} of BC2 and the L2-linac rf phase can be adjusted, we typically only adjust the linac rf phase to change the compression ratio. Figure 2 shows a chirp scan at hard x-ray energy. We recorded the FEL pulse energy and BC2 bunch length monitor (BLM) signal. In this figure, the e-beam is under-compressed at the right side. At about -32.2°, the bunch gets fully compressed with a peak current signal. After full compression, at the left side of this figure, the bunch is over-compressed, and the peak current goes down. The FEL pulse energy has two humps during the chirp scan, one at the under-compression side, and the other one at the over-compression side. Note even at full-compression, the FEL still survives, but the pulse energy is dropped to about 20 μJ. This dip is probably due to a very short pulse duration and other collective effects such as CSR. Simulation indicates that an x-ray pulse duration of about 1 fs fwhm can be obtained at full-compression mode, which means the x-ray peak power is still about 20 GW even with only 20uJ pulse energy.

It is interesting that we still have FEL lasing at full compression, where a very short e-beam and x-ray pulses could be generated. We measured the FEL power gain length of 2.7m at the full-compression mode, as shown in Fig. 3. The measured intensity fluctuation is about 11-13% at under- or over-compression side, and about 25% at full-compression

* Work supported by the Department of Energy under Contract Number: DE-AC02-76SF00515.
† Current address: LBNL, Berkeley, CA 94720, USA.

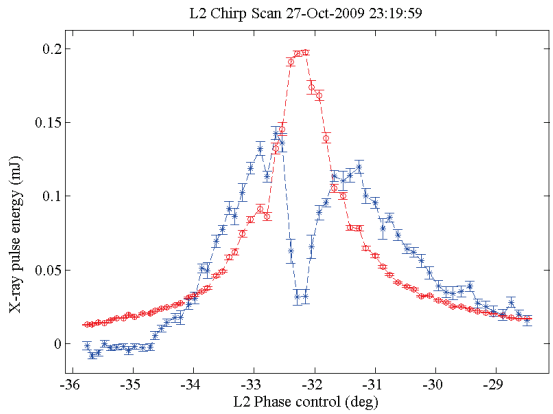

Figure 2: Hard x-ray (1.5Å) pulse energy (blue stars) and BC2 current (red circles, arb. units) vs. L2 RF phase (zero is on-crest).

mode. At BC2 full-compression mode, we can further adjust the L1 phase to get less compression in BC1. Then a smaller uncorrelated energy spread before BC2 could help achieve a shorter pulse duration [5].

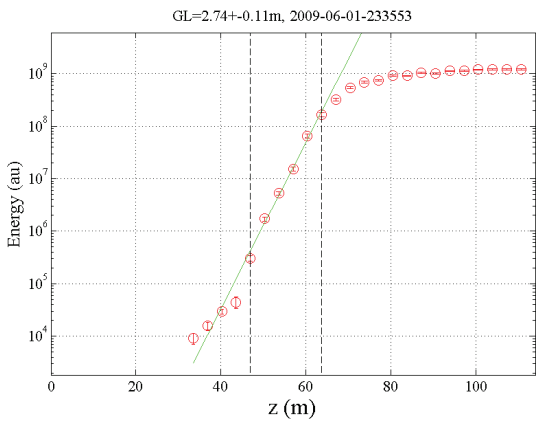

Figure 3: Hard x-ray (1.5 Å) power gain curve measurement at full compression with 20pC.

Soft x-ray FELs at 20pC

At soft x-ray wavelength, a similar L2 chirp scan is shown in Fig. 4 at 1.5 nm. At this photon wavelength, it is clear that there is no lasing at full-compression. This lasing suppression at full-compression is mainly due to the large relative energy spread and also the FEL slippage at this wavelength.

Some user experiments have indicated a pulse duration of less than 10 fs at under- or over-compression with 20pC [3]. To achieve an even shorter or single-spike x-ray pulse, we can combine the slotted foil (to be discussed in the following section) with low charge. Simulation studies can be found in [5]. This has been also studied with SXR spectral measurements [6]. Further reducing the charge to a few pC could also help get a shorter x-ray pulse [7].

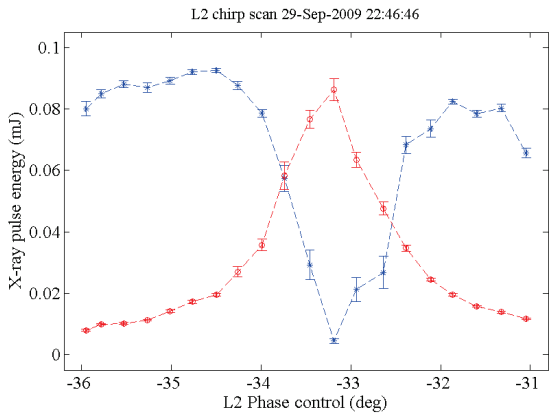

Figure 4: Soft x-ray (1.5nm) pulse energy (blue stars) and BC2 current (red circles, arb. units) vs. L2 RF phase (zero is on-crest).

SLOTTED-FOIL OPERATION

Another method for femtosecond pulse generation is to use an emittance-spoiling foil (a slotted foil), which was first proposed in 2004 [8] and has been on-line at the LCLS since 2010. While the dispersed electron beam passes through a foil with a single or double slots, most of the beam emittance will be spoiled, leaving very short unspoiled time slices to produce femtosecond x-rays.

To achieve a variable pulse duration and separation, an aluminum foil (3 μm thickness) with different slot arrays was designed. The present design includes a vertical V-shape single slot with a variable slot width (220-1580 μm), and two V-shape double slots with different slot separation at two fixed slot widths (300 and 430 μm), as shown in the bottom of Fig. 5. The choice of these slot sets were determined by the user interests, FEL performance and also the practical considerations of manufacturing. The double-slot setup enables x-ray pump/x-ray probe experiments. We show in Fig. 5 an example of the measured x-ray pulse energy vs. foil vertical position, at photon energy 1.5keV and bunch charge 150pC [9].

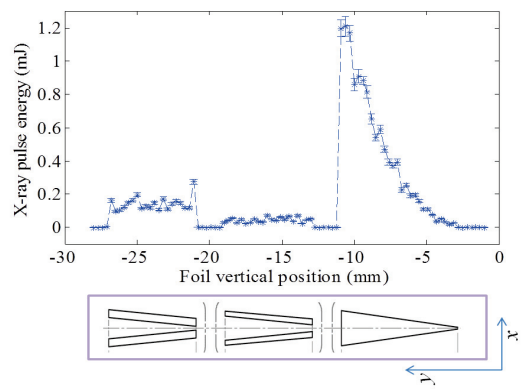

Figure 5: Measured FEL pulse energy vs. foil vertical position. The slot arrays are shown at the bottom [9].

ISBN 978-3-95450-122-9

For a double-slotted foil with a slot separation Δd (center to center), we will get two unspoiled electron beams, and their temporal separation after the chicane can be calculated by:

$$\Delta t = \frac{\Delta d}{\eta h C c}. \quad (1)$$

C is the compression factor in the chicane, η is the dispersion at the foil location, h is the time-energy chirp before the chicane, and $c = 3 \times 10^8 m/s$ is the speed of light. Similarly, we can also calculate the pulse duration from a single slot with a finite width, but the uncorrelated energy spread $\sigma_{\delta 0}$ and betatron beam size ($= \sqrt{\epsilon\beta}$) have to be included. As discussed in [10], the FWHM duration of the unspoiled portion of the electron bunch is given by

$$\Delta\tau = \frac{2.35}{\eta h c}\sqrt{\eta^2\sigma_{\delta 0}^2 + (1 + hR_{56})^2(\Delta x^2/3 + \epsilon\beta)}. \quad (2)$$

Here Δx is the half slot width, and R_{56} is the chicane momentum compaction. The main difficulty in the calculations is to know the initial beam chirp h. In the calculations, we use the bunch lengths before (σ_{z1}) and after the chicane (σ_{z2}) measured from BLMs to determine this chirp:

$$h = \left(1 - \frac{\sqrt{\sigma_{z2}^2 - R_{56}^2\sigma_{\delta 0}^2}}{\sigma_{z1}}\right)/|R_{56}|. \quad (3)$$

At 150pC bunch charge, we calculated the pulse duration (fwhm) from the single-slotted foil and the pulse separation (delay) from the double-slotted foil, as shown in Table.1. In these calculations, the initial bunch length in injector is 420 μm, energy spread after laser heater is 20keV and BC1 peak current is 220A. $R_{56} = -24.7$mm, and $\eta = -362.1$mm. The measured pulse delays based on a cross-correlation method agree reasonably well with these calculations [9].

Table 1: Calculated pulse duration/separation at 150pC.

	single slot, dur. $\Delta\tau$		double slots, delay Δt	
BC2	min(fs)	max(fs)	min(fs)	max(fs)
1kA	12.8	56.9	36.3	79.2
2kA	7.4	25.8	16.2	35.2
3kA	6.1	17.0	10.3	22.6

DIAGNOSTICS DEVELOPMENT

Diagnostics at low-charge mode and slotted-foil case is very challenging. The available diagnostic devices at LCLS were designed with a resolution for high-charge operation mode. For example, the present TCAV3 resolution is about 10 fs rms, and most of the BPMs work fine at 10-20pC, but it is challenging for even lower charges. A general review of the present diagnostics can be found in [11]. To achieve a better resolution for temporal diagnostics, several schemes have been recently developed: statistical method, longitudinal mapping with A-line, wide-band THz spectrometer, e-beam and x-ray cross-correlation, and X-band rf transverse deflector.

The statistical method is developed based on the spectral correlation function analysis[12]. The longitudinal mapping technique involves adjusting the LCLS second bunch compressor followed by running the bunch on an rf zero-crossing phase of the final 550-m of linac. As a result, the time coordinate of the bunch is directly mapped onto the energy coordinate. This technique has been benchmarked with TCAV3, and a minimum rms bunch length of less than 1fs has been measured at 20pC. [13]. A single-shot, THz prism spectrometer in DL2 area has been built, which collects coherent transition radiation from an aluminum foil. The designed system covers a spectral range of 1.2 - 40 micrometer. Experimental progress has been made to reconstruct the e-beam temporal profile using the Kramers-Kronig phase retrieval method [14]. The self-seeding chicane at LCLS enables the e-beam and x-ray cross-correlation measurements. The chicane washes out the e-beam microbunching and also delays the e-beam. By recording the final x-ray pulse intensity vs. the relative delay, the x-ray pulse duration can be obtained [9]. An X-band rf transverse deflector has been also installed at the end of the LCLS undulator beamline, and commissioning is just started [15]. This deflector is designed to measure the longitudinal phase space of the electron beam with a temporal resolution down to a few fs. Since it is located after the undulator, we can analyze the difference between lasing and non-lasing beams, from which the x-ray temporal profile could be retrieved.

REFERENCES

[1] P. Emma et al., Nat. Photon. 4, 641 (2010).

[2] Y. Ding et al. Phys. Rev. Lett. 102, 254801 (2009).

[3] e.g., M. Hoener et al., Phys. Rev Lett. 104, 253002 (2010); R. Coffee, private discussion.

[4] R. Iverson et al, to be presented at FEL13, New York (2013).

[5] L. Wang, Y. Ding, Z. Huang, IPAC11, p3131, Spain (2011).

[6] G. Williams, private discussion.

[7] V. Wacker et al., FEL12, THPD31, Japan (2012).

[8] P. Emma et al., Phys. Rev Lett. 92, 074801 (2004).

[9] Y. Ding et al., Phys. Rev Lett. 109, 254802 (2012).

[10] P. Emma, Z. Huang and M. Borland, FEL04, p333, Italy (2004).

[11] J. Frisch et al., BIW08, p17, USA (2008); H. Loos et al., BIW10, p34, USA (2010); H. Loos, SPIE conference, Proc. 8778-18, Czech Republic (2013);

[12] A. A. Lutman et al., Phys. Rev. ST Accel. Beams 15, 030705 (2012);

[13] Z. Huang et al., Phys. Rev. ST Accel. Beams 13, 092801 (2010); Z. Huang et al., PAC11, p. 2459.

[14] T. Maxwell et al., IBIC12, TUPA47, Japan (2012).

[15] Y. Ding et al., Phys. Rev. ST Accel. Beams 14, 120701 (2011); P. Krejcik et al., THPB01 in IBIC12, Japan (2012); Y. Ding et al. WEOBB201 in this conference.